Fan and Pump Efficiency in Modelica based on the Euler Number

Hongxiang Fu[1] David Blum[1] Michael Wetter[1]

[1]Building Technology and Urban Systems Division, Lawrence Berkeley National Laboratory, USA,
{hcasperfu,dhblum,mwetter}@lbl.gov

Abstract

Simulation programs often assume constant hydraulic efficiency for fan or pump models when performance curves are unavailable. This is inaccurate because the hydraulic efficiency varies with the operation condition. It therefore consistently underestimates the power draw at off-design conditions at which the hydraulic efficiency drops. Use of a modified Euler number allows computing the hydraulic efficiency and shaft power with limited data. Others showed the validity of the modified Euler number for fan efficiency calculations. We show that it is also applicable for pumps, and present its implementation in Modelica for a fan or pump model. The only input required from the user is one data point at which the hydraulic efficiency is at its maximum. The reported method is applicable regardless of the type, size, or operational region of the fan or pump. Across a sample of eighteen sets of pump data and seven sets of fan data, the errors of the computed power from interpolated data were within 15% for the range of 20% - 70% of maximum flow rate and 40% - 90% of maximum pressure rise, excluding outliers.

Keywords: fan efficiency, pump efficiency, component model

1 Introduction

Movers (fans and pumps) are important components in building energy systems and the accuracy of their component models are pertinent to the accuracy of the energy model as a whole. Often of particular interest is the calculation of power consumption, which in reality is a function of mover fluid volume flow rate $\dot{V}$, pressure rise Δp, hydraulic efficiency η_{hyd}, and motor efficiency η_{mot}, shown by

$$P = \frac{\dot{V}\,\Delta p}{\eta_{hyd}\,\eta_{mot}}. \tag{1}$$

Note that the flow work is simply

$$\dot{W}_{flo} = \dot{V}\,\Delta p \tag{2}$$

and the hydraulic work, $\dot{W}_{hyd}$, is the mechanical work transmitted to the shaft of the mover to provide such flow work with a hydraulic efficiency as

$$\dot{W}_{hyd} = \frac{\dot{W}_{flo}}{\eta_{hyd}}. \tag{3}$$

The hydraulic efficiency is itself a function of volume flow rate and pressure rise. Calculating power accurately for a broad range of operating conditions and system configurations, therefore, requires both explicit calculation of volume flow rate and pressure rise as well as correct characterisation of efficiency as their function.

Conventional building energy modeling programs do not explicitly calculate both volume flow rate and pressure rise. Therefore, they rely on similarity laws or polynomial regressions that calculate power as a function of flow rate only, implicitly making assumptions about system pressure characteristics and mover efficiency. One particular danger in this approach was pointed out by Englander and Norford (1992a) in the case of static pressure-controlled fans, a typical application for variable air volume (VAV) supply fans common in U.S. commercial HVAC systems. There, Englander and Norford (1992a) showed that, because a static pressure-controlled fan will maintain a pressure rise even at very low flow, power consumption does not trend to zero as the flow rate trends zero. The similarity laws and flow rate regression polynomials with this assumption therefore do not hold. Their data showed this could lead to underestimation of fan power consumption in cases without static pressure reset strategies. Consider also that in a typical fan performance map, shown in Figure 1, the power consumption (indicated by BHP) is non-zero at zero flow or non-zero pressure rise. Therefore, these authors proposed a revised polynomial formulation of power as a function of flow and static pressure set point in a separate paper (Englander and Norford 1992b). Such a correlation utilized an offset term determined by static pressure set point for when flow approaches zero. Similar correlations were suggested by Hydeman et al. (2003).

Such curves can be implemented by the user in simulation software such as EnergyPlus (U.S. DOE 2021), Trace (The Trane Company 2019), and IDA-ICE (EQUA Simulation AB 2013). However, because this still requires the user to have some information on the mover and the system, users often use the default curve provided by the program. One commonly used default curve comes from ASHRAE Standard 90.1 Table G3.1.3.15 (ASHRAE

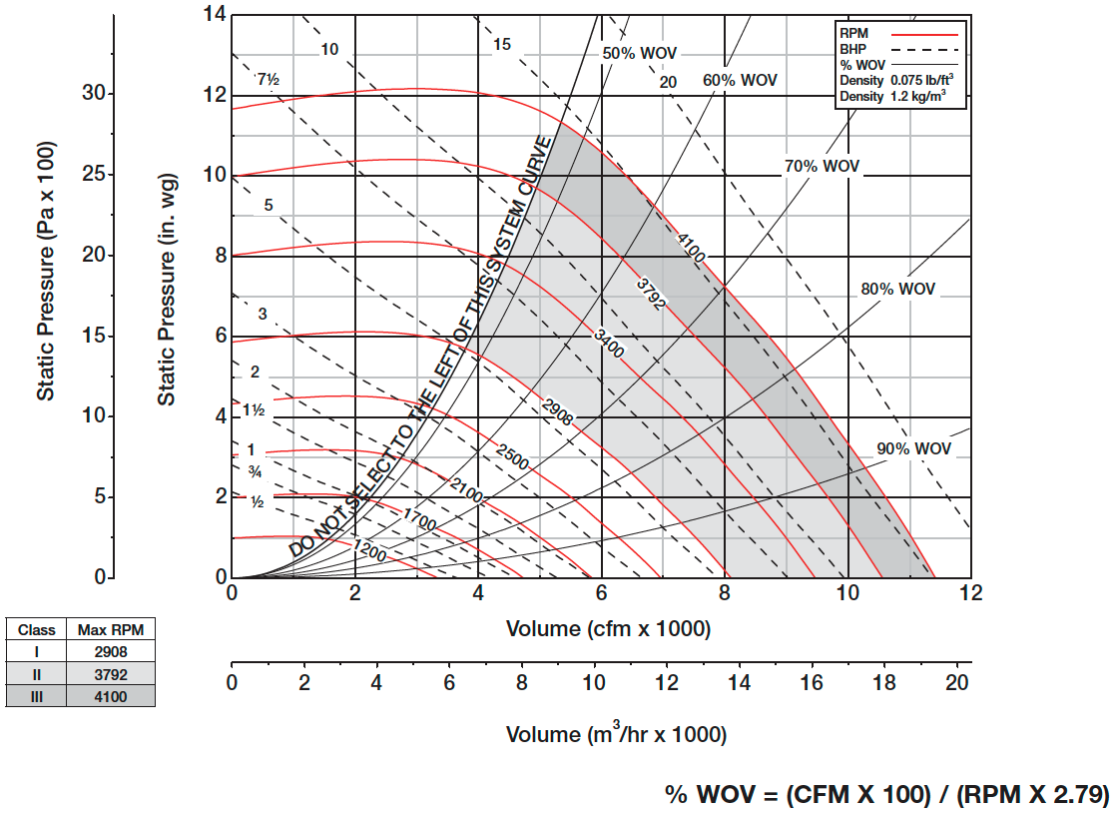

Class	Max RPM
I	2908
II	3792
III	4100

Figure 1. An example of fan curves from the manufacturer. Greenheck Fan Corporation (2012), reproduced as is.

2020) which takes the form

$$P/P_d = 0.0013 + 0.1470\,PLR + 0.9506\,PLR^2 - 0.0998\,PLR^3, \quad (4)$$

where P_d is the fan power at design condition and PLR is the flow part load ratio

$$PLR = \dot{V}/\dot{V}_d, \quad (5)$$

where $\dot{V}_d$ is the design flow rate. With this correlation, the computed power still effectively trends to zero when the flow rate goes to zero.

While the polynomial regressions represent improvements over the basic similarity laws, they do not generalize to any mover or system and control configuration where more detailed performance and operating state may be known through specific mover performance maps and explicit simulation of the pressure-flow network and controls. Modelica-based modeling has enabled such explicit network and controls simulation. However, the ability to represent the whole mover performance map fully and conveniently is lacking. This includes accounting for the complex variations in efficiency, especially with low flows and significant pressure rise, as would be the operating region of movers operating to maintain a pressure set point with little or no reset based on load. Here, low efficiency likely accounts for significant non-zero power consumption as $\dot{V}$ reduces to zero in (1).

Therefore, in this paper, we report a Modelica implementation of a convenient method to represent mover performance with such accuracy. It only requires the user to provide one data point of η, $\dot{V}$, and Δp where the efficiency is at its maximum. The method then uses a dimensionless modified Euler number and a correlation to estimate the efficiency and power at any operation point. This method is applicable regardless of the type, size, or operational region (stall or non-stall) of the mover. This method is valuable because it provides the analyst with more accurate estimation of mover shaft power while requiring only limited information. It thus is applicable at early stages of design or post-retrofit assessment during which detailed mover performance data are generally not available.

2 Methodology

2.1 Efficiencies

Manufacturers often provide fan or pump performance curves describing how its hydraulic power $\dot{W}_{hyd}$ (often denoted as "shaft power" or "brake horsepower") depends on $\dot{V}$, Δp, and mover speed N. $\dot{W}_{hyd}$ differs from $\dot{W}_{flo}$ by

 10.3384/ECP2118619 DOI

a factor of hydraulic efficiency as shown in (3) and from the total electric power drawn by the mover P by motor efficiency

$$\eta_{mot} = \dot{W}_{hyd}/P. \tag{6}$$

The total efficiency η can then be expressed as the product of the two

$$\eta = \eta_{hyd}\,\eta_{mot}. \tag{7}$$

The implemented method is based on $\dot{W}_{hyd}$ and η_{hyd}. However, in this paper, we also applied this method for P and η as this was the type of pump data available to us. For simplicity, the remainder of this work will use η^* to denote either η or η_{hyd} and P^* to denote either P or $\dot{W}_{hyd}$. Through Figure 2 we will show that this assumption has worked well with our data. We note that U.S. DOE (2014) shows that η_{mot} is mostly constant for motors larger than about 3.5 kW (around 5 HP) except when the motor part load drops below around 40%. To accommodate applications with small motors or large operating regions, our implementation of the model allows the user to specify a separate function for the motor efficiency.

2.2 Modified Euler Number

The Euler number is defined for any medium as

$$Eu = \frac{\text{pressure forces}}{\text{inertial forces}}. \tag{8}$$

This can be written as

$$Eu = \frac{\Delta p A}{p_d A} = \frac{\Delta p}{p_d}, \tag{9}$$

where p_d is the dynamic pressure and A is a characteristic area. The dynamic pressure is

$$p_d = \frac{v^2\rho}{2} = \frac{\dot{V}^2\rho}{2A^2}, \tag{10}$$

where v is the velocity, which is proportional to the volumetric flow rate. Substituting (10) into (9) yields

$$Eu = \frac{2\Delta p A^2}{\rho\dot{V}^2}. \tag{11}$$

U.S. DOE (2021) and Haves et al. (2014) reported a model in EnergyPlus that describes these multidimensional relationships of fans. The model is based on two steps: First, it expresses the fan performance using a non-dimensional equation that is derived from the Euler number as

$$Eu^* = \frac{\Delta p D^4}{\rho\dot{V}^2}, \tag{12}$$

where Eu^* is the modified Euler number, D is the fan wheel outer diameter, and ρ is the medium density at the mover inlet. Because D is constant for the same fan and ρ is approximately constant across the operating region in HVAC applications, the ratio of the modified Euler number can be expressed as

$$\frac{Eu^*}{Eu^*_p} = \frac{\Delta p}{\dot{V}^2}\frac{\dot{V}_p^2}{\Delta p_p}, \tag{13}$$

where the subscript p denotes the peak operation point at which η_{hyd} attains its maximum, and the quantities without subscript are any operating point.

Second, it expresses the ratio of hydraulic efficiency $\eta_{hyd}/\eta_{hyd,p}$ using an exponential-conditioned skew-normal function that takes the ratio of the modified Euler number Eu^*/Eu^*_p as an argument. U.S. DOE (2021) shows that this relationship is remarkably similar across different fan sizes and types, both within the stall and non-stall regions. The normalized exponential-conditioned skew-normal function is

$$\frac{\eta_{hyd}}{\eta_{hyd,p}} = \frac{\exp(-0.5Z_1^2)\left(1+\frac{Z_2}{|Z_2|}\operatorname{erf}\left(\frac{|Z_2|}{\sqrt{2}}\right)\right)}{\exp(-0.5Z_3^2)\left(1+\frac{Z_3}{|Z_3|}\operatorname{erf}\left(\frac{Z_3}{\sqrt{2}}\right)\right)}, \tag{14}$$

where

$$Z_1 = (x-a)/b, \tag{15}$$
$$Z_2 = (\exp(cx)\,dx-a)/b, \tag{16}$$
$$Z_3 = -a/b, \tag{17}$$
$$x = \log_{10}(Eu^*/Eu^*_p), \tag{18}$$

and

$$a = -2.732094, \tag{19}$$
$$b = 2.273014, \tag{20}$$
$$c = 0.196344, \tag{21}$$
$$d = 5.267518. \tag{22}$$

Note that with this formulation, the user merely needs to provide values for $\dot{V}_p$, Δp_p and $\eta_{hyd,p}$, from which η_{hyd} can be solved for any operating condition.

U.S. DOE (2021) and Haves et al. (2014) discussed this similarity in the context of fan but not pumps. But from (11) and (12) it follows that

$$\frac{Eu}{Eu_p} = \frac{Eu^*}{Eu^*_p}. \tag{23}$$

From (23), we conclude that (13) is applicable regardless of medium, thus it is also applicable for pumps. Next, it remains to be shown that the empirical relation (14) is also applicable for pumps. In Figure 2 we overlaid operating points of fans and pumps to the empirical relation (14). As can be seen from the figure, pump operation points also match the empirical relation (14). To the best of our knowledge, this is the first report that shows the validity of (14) for pumps. Further validation based on the model that is described in Section 3 is given in Section 4.

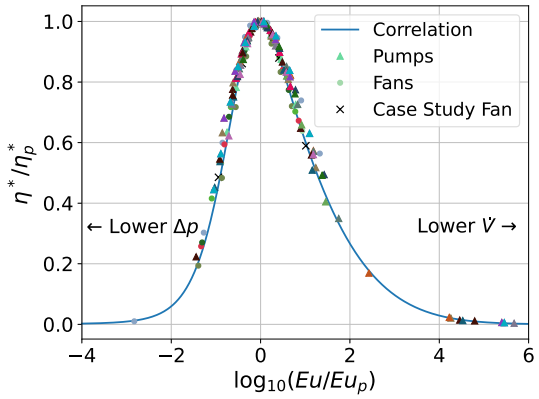

Figure 2. Normalized efficiency curves in dimensionless space and mover performance data. Each colour represents one dataset of seven fan models and eighteen pump models.

3 Modelica Implementation

The `Buildings.Fluid.Movers` package (Wetter 2013) of the Modelica Buildings Library (Wetter et al. 2014) was revised to implement the reported method. The revised model is available through commit 346f5a0 and will be released in future versions of the Modelica Buildings Library. In the previous model, the user could provide either data for $P = f(\dot{V})$, or data for $\eta_{hyd} = f(\dot{V})$ and $\eta_{mot} = f(\dot{V})$. The new implementation separated the computation of the three efficiency terms, η, η_{hyd}, and η_{mot}, allowing a user to specify two such that the third is computed by Equation 7. The efficiency η^* and the power P^* are pre-computed using the Euler number to construct two 2D look-up tables that are implemented using `Modelica.Blocks.Tables.CombiTable2Ds`. These two variables are then found through two-dimensional interpolation during the simulation. There are a number of rationales for this approach:

1. Storing pre-computed values avoids having to evaluate (14) at each time step. This is preferable especially because (14) is computationally expensive and not globally differentiable.

2. As can be seen from (18), both Δp and $\dot{V}$ must be bounded away from zero to avoid the logarithm at zero and the division by zero. This is more easily managed when the power and efficiency are pre-computed.

3. As can be seen in Figure 2, in (18) and in (13), $\eta_{hyd} \to 0$ when either $\Delta p \to 0$ or $\dot{V} \to 0$. This would cause the computed power P to approach infinity. Again, this is more easily avoided by using pre-computed tabulated values.

To construct the tables, the support points are computed from (14) in 10% equidistant increments as

$$\{\Delta p_i\}_{i=0}^{10} = \{\Delta p_{max}\, i/10\}_{i=0}^{10}, \tag{24}$$

where $\Delta p_{max} = \Delta p(\dot{V} = 0, n = 1)$ and n is the normalized speed, and similarly

$$\{\dot{V}_i\}_{i=0}^{10} = \{\dot{V}_{max}\, i/10\}_{i=0}^{10}, \tag{25}$$

where $\dot{V}_{max} = \dot{V}(\Delta p = 0, n = 1)$. The efficiency η^* at boundary points ($\Delta p = 0$ or $\dot{V} = 0$) is set to zero. The power P^* at these boundary points is extrapolated except at $\Delta p = 0$ and $\dot{V} = 0$ where it is set to zero.

4 Validation

We validated the implemented method by comparing the model output of η^* and P^* against values interpolated from performance maps. The peak performance data Δp_p, $\dot{V}_p$, and η_p were obtained from the mover curve at maximum speed. They are then used by the model to compute the look-up tables. The efficiency and power as computed by the model were then compared to the original performance curves. It is important to note that although full performance curves were used here to find the peak point for the purpose of this validation, the user only needs to provide the peak point to use the model.

4.1 Nominal Speed

Figure 3 shows the validation results using the performance curve at nominal speed $N = 4100$ rpm in Figure 1. The computed efficiency and power are compared against values interpolated from the performance map. Figure 3(e) shows that the fan reproduces the pressure curve at a constant speed. As can be seen from Figure 3(a) and Figure 3(b), the computed efficiency closely follows the values from the performance map for the full range of $\dot{V}$ and Δp. The computed power is also accurate for most of the range but the two curves diverged slightly at high $\dot{V}$ and more so at low Δp. Power values computed from constant efficiencies are plotted through the grey shaded region. When the efficiency was assumed constant at its peak value of $\eta_{hyd} = 0.68$, the computed power was always underestimated. As expected, when a lower value of $\eta_{hyd} = 0.46$ is used for the constant efficiency, the computed power was overestimated in some region and underestimated in some other, as reported by Englander and Norford (1992a). Either way, if a constant efficiency is used, the power goes to zero as the flow approaches zero, which is physically incorrect if the mover continues to create pressure rise.

Figure 4 shows the errors from a sample of eighteen sets of pump data and seven sets of fan data. First, the distributions of the errors are almost all skewed to the same direction in each subplot. The errors of η^* have tails on the negative side at high $\dot{V}$ and low Δp and the errors of P^* are skewed to the opposite direction. Second, with the outliers and boxes at extreme $\dot{V}$ or Δp values put aside, the errors are all roughly within 20%. If the threshold is tightened to 15%, this method provided satisfactory results for η in the range of 20% - 80% of $\dot{V}_{max}$ and 30% - 90% of Δp_{max}, and for P in the range of 20% - 70% of $\dot{V}_{max}$ and 40% - 90% of Δp_{max}, excluding outliers.

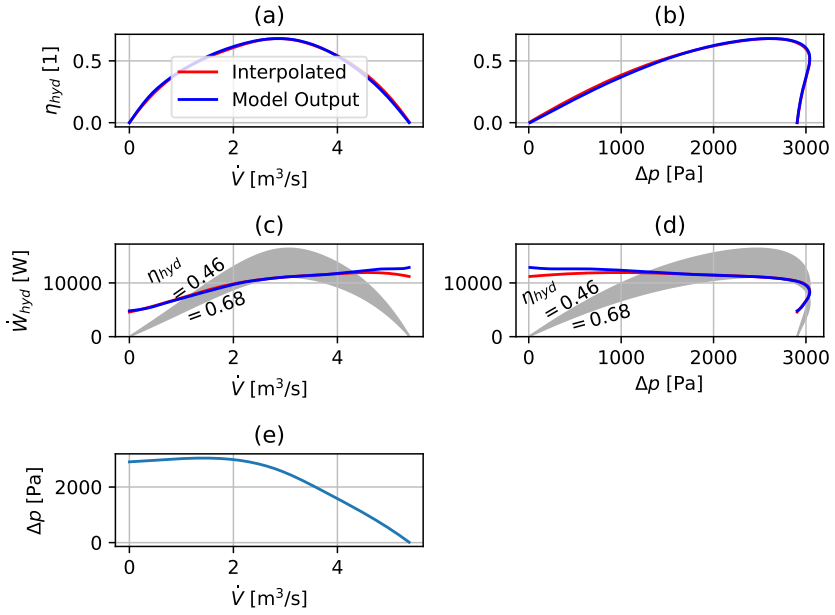

Figure 3. Hydraulic efficiency and power values that were interpolated from the performance map (red lines) and computed by the model (blue lines). The grey shaded area is bounded by the simplified assumption of a constant hydraulic efficiency between $\eta_{hyd} = 0.68$ (peak of this fan) and $\eta_{hyd} = 0.46$ and shown here to visualize the wrong results of this oversimplification.

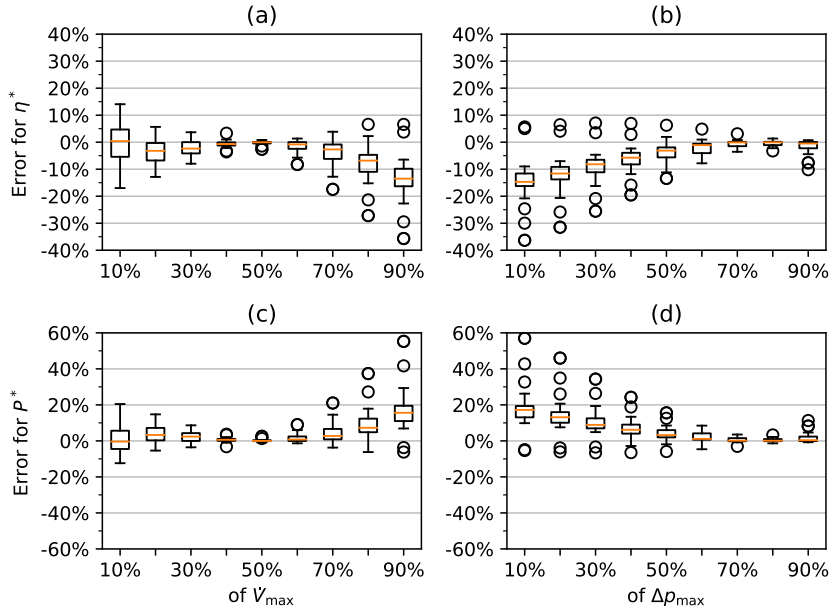

Figure 4. Box-whisker plots for errors of computed efficiency and power against values interpolated from performance maps. The sample consists of eighteen sets of pump data and seven sets of fan data. The middle lines in the boxes correspond to the medians. The outliers are defined as points more than 1.5 interquartile ranges away out from the maximum or the minimum.

4.2 Reduced Speed

We also validated the method for reduced speed. Figure 5 shows the power computed by the implemented method compared to interpolated values at three different speeds. The interpolation was done from Figure 1 at $N = 4100$ RPM ($n = 1$), 3400 RPM ($n = 0.83$), and 2500 RPM ($n = 0.61$). The figure shows that the error patterns are remarkably similar across the different speeds.

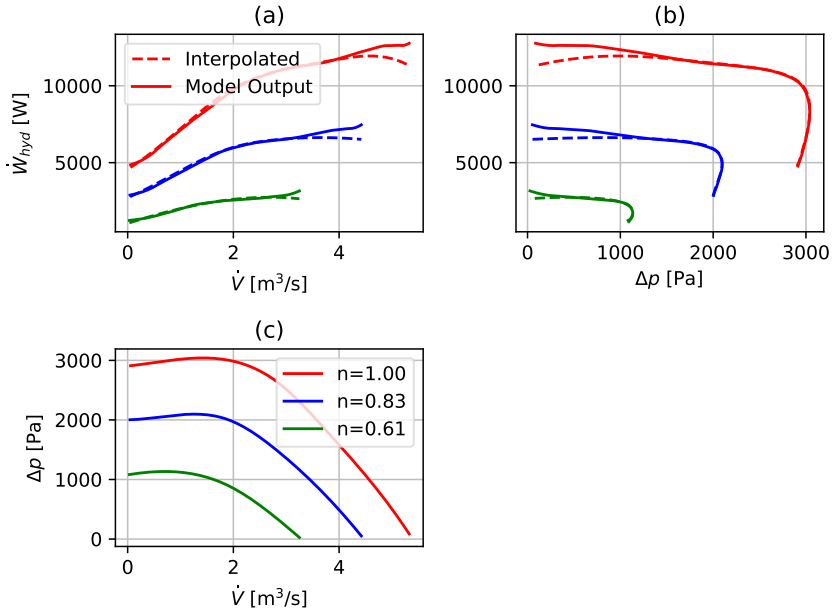

Figure 5. Hydraulic power values that were interpolated and that were computed by the model at nominal ($n = 1$) and reduced ($n < 1$) speeds.

5 Discussion

Figure 4 shows that the error distributions within each subplot are skewed to the same direction. The errors of η^* are consistently negative. This is likely caused by the fact that the global maximum of efficiency is above the curve of maximum speed, which leads to η_p^* being underestimated. Because η^* is computed based on η_p^*, η^* will also be consistently underestimated. Consequently, the errors of P^* are skewed to the positive side as $P^* \propto 1/\eta^*$.

Figure 5 suggests that, when compared to the manufacturer data, the increased discrepancies of $\dot{W}_{hyd}$ mostly occur at the lower right region of the fan performance map. A properly-sized fan or pump should operate somewhere near the midpoint on its nominal speed curve at full load. At reduced load, its operating point moves to the left because of reduced flow. A mover is therefore unlikely to operate in this region in which the discrepancy is the largest.

Besides η_{hyd}, the implementation allows the user to specify η_{mot} as well, although the part-load behaviour of η_{mot} is beyond the scope of this work.

We note that the Euler method does not reproduce efficiency degradation along constant system curves, e.g., along the curves $\Delta p = k\dot{V}^2$, for any constant $k \geq 0$. This limitation follows from (14), which has the functional form

$$\begin{aligned} \frac{\eta_{hyd}}{\eta_{hyd,p}} &= f(x) = f\left(log_{10}(Eu^*/Eu_p^*)\right) \\ &= f\left(\log\left(\frac{\Delta p}{\dot{V}^2}\frac{\dot{V}_p^2}{\Delta p_p}\right)\right). \end{aligned} \tag{26}$$

As $\dot{V}_p^2$ and Δp_p are constants, the functional dependency (26) can be further reduced to

$$\frac{\eta_{hyd}}{\eta_{hyd,p}} = g\left(\frac{\Delta p}{\dot{V}^2}\right). \tag{27}$$

Therefore, the efficiency η_{hyd} is constant along any curve $\Delta p = k\dot{V}^2$, and it remains at its peak along the curve for which $k = \Delta p_p/\dot{V}_p^2$. This is in line with the simplification often used by fan manufacturers to generate fan curves at different speeds (Stein and Hydeman 2004) and this simplification is explicitly permitted by ASHRAE Standard 51-16 (ANSI/AMCA Standard 210-16) (ASHRAE 2016). For this reason, fan or pump performance maps whose reduced-speed performance is measured are difficult to find. Turbines share similar fluid-flow principals to fans and pumps and their performance maps often display contours of constant efficiency that suggest that there is no constant efficiency line along such a quadratic curve (e.g. Leylek (2012) and Garrett Motion (2019)).

This further indicates that the Euler number method is less accurate than using the measured data at reduced speed. However, such measured data are rare for fans or pumps. In this case the reported method has the same accuracy in theory and it would depend on whether the user finds it more convenient to only use one data point of peak operation instead of entering a whole curve into the model. Still, it is important to emphasize that the Euler number method is implemented to help with the situation where the mover data are unavailable.

6 Conclusion

This work describes the Modelica implementation of a method that computes fan or pump efficiency and power using the dimensionless Euler number. With this method, the only input required from the user is the flow rate, pressure rise, and hydraulic efficiency at the peak operation point where the hydraulic efficiency is at its maximum. This practice is valuable because it provides the user with an accurate computation that requires only limited data, and it does not suffer from the errors that occur if a constant efficiency is used.

The implemented method was validated with seven sets of fan and eighteen sets of pump data obtained from manufacturers. Across the sample and between the values computed from the reported method and from interpolation of manufacturer data, the errors of efficiency were within 15% in the range of 20% - 80% of $\dot{V}_{max}$ and 30% - 90% of Δp_{max}, excluding outliers. The errors in power were within 15% in the range of 20% - 70% of $\dot{V}_{max}$ and 40% - 90% of Δp_{max}, excluding outliers. The errors were larger when $\dot{V}$ was high or when Δp was low. These discrepancy patterns remained largely the same at reduced speeds. Because the increased discrepancies mostly occurred in a region in which a properly-sized mover is unlikely to operate, they have little effect on the accuracy of this method compared to using manufacturer data in common HVAC applications.

The paper shows how an underestimated peak efficiency introduces consistent and systematic errors. Improving the methodology for finding the peak efficiency on the manufacturer-provided power map would increase the accuracy of the model. Furthermore, more uncertainty analysis is needed to understand how the errors of the estimation of the peak point influence the errors of the computed efficiency and power. Understanding the uncertainty is important for this application because it is intended to be used when the user has limited information and must make reasoned estimations.

Acknowledgements

This research was supported by the Assistant Secretary for Efficiency and Renewable Energy, Office of Building Technologies of the U.S. Department of Energy, under Contract No. DE-AC02-05CH11231.

This work emerged from the IBPSA Project 1, an international project conducted under the umbrella of the International Building Performance Simulation Association (IBPSA). Project 1 will develop and demonstrate a BIM/GIS and Modelica Framework for building and community energy system design and operation.

References

ASHRAE (2016). *ASHRAE Standard 51-16 (ANSI/AMCA Standard 210-16), Laboratory Methods Of Testing Fans For Certified Aerodynamic Performance Rating*. ASHRAE.

ASHRAE (2020). *ANSI/ASHRAE/IES Standard 90.1-2019: Energy Standard for Buildings Except Low-Rise Residential Buildings*. ASHRAE.

Englander, SL and LK Norford (1992a). "Saving fan energy in VAV systems- part 1: analysis of a variable-speed-drive retrofit." In: *ASHRAE Winter Meeting, Anaheim, CA, USA, 01/25-29/92*, pp. 3–18.

Englander, SL and LK Norford (1992b). "Variable Speed Drives: Improving Energy Consumption Modeling and Savings Analysis Techniques." In: *Proc. of the ACEEE Summer Study 1992*, pp. 3.61–3.78.

EQUA Simulation AB (2013-02). *User Manual: IDA Indoor Climate and Energy Version 4.5*. Date accessed: 31-Mar-2022. URL: http://www.equaonline.com/iceuser/pdf/ice45eng.pdf.

Garrett Motion (2019). *Turbo Tech 103 | Expert: Compressor Mapping*. Date accessed: 29-Aug-2022. URL: https://www.garrettmotion.com/wp-content/uploads/2019/10/GAM_Turbo-Tech-103_Expert-1.pdf.

Greenheck Fan Corporation (2012). *Double-Width Centrifugal Fan Performance Supplement*. Date accessed: 2-Dec-2021. URL: https://content.greenheck.com/public/DAMProd/Original/10002/CentrifugalDWPerfSuppl_catalog.pdf.

Haves, Philip et al. (2014-09). *Development of Diagnostic and Measurement and Verification Tools for Commercial Buildings*. Tech. rep. CEC-500-2015-001. Lawrence Berkeley National Laboratory.

Hydeman, Mark et al. (2003-10). *Advanced VAV System Design Guide*.

Leylek, Zafer (2012-10). *An Investigation into Performance Modelling of a Small Gas Turbine Engine*. Tech. rep. DSTO-TR-2757. Defence Science and Technology Organisation. URL: https://www.dst.defence.gov.au/sites/default/files/publications/documents/DSTO-TR-2757.pdf.

Stein, Jeff and Mark Hydeman (2004). "Development and Testing of the Characteristic Curve Fan Model." In: *ASHRAE transactions* 110.1.

The Trane Company (2019-02). *TRACE 600 Engineering Manual*. Date accessed: 31-Mar-2022. URL: https://tranecds.custhelp.com/ci/fattach/get/120633/0/filename/TRACE_600_Engineering_Manual%5C%5B1%5C%5D.pdf.

U.S. DOE (2014-04). *Determining Electric Motor Load and Efficiency*. Date accessed: 10-Mar-2022. URL: https://www.energy.gov/sites/prod/files/2014/04/f15/10097517.pdf.

U.S. DOE (2021-09). *EnergyPlus Version 9.6.0 Documentation: Engineering Reference*. Date accessed: 2-Dec-2021. URL: https://energyplus.net/assets/nrel_custom/pdfs/pdfs_v9.6.0/EngineeringReference.pdf.

Wetter, Michael (2013-08). "Fan and Pump Model That Has a Unique Solution for Any Pressure Boundary Condition and Control Signal". In: *Proc. of the 13th Conference of the International Building Performance Simulation Associationn*. Chambéry, France, pp. 3505–3512.

Wetter, Michael et al. (2014). "Modelica Buildings Library". In: *Journal of Building Performance Simulation* 7.4, pp. 253–270.